

# CARTOS: A Charging-Aware Real-Time Operating System for Intermittent Batteryless Devices

Mohsen Karimi, Yidi Wang, Youngbin Kim, Yoojin Lim, Hyoseung Kim,

**Abstract**—This paper presents CARTOS, a charging-aware real-time operating system designed to enhance the functionality of intermittently-powered batteryless devices (IPDs) for various Internet of Things (IoT) applications. While IPDs offer significant advantages such as extended lifespan and operability in extreme environments, they pose unique challenges, including the need to ensure forward progress of program execution amidst variable energy availability and maintaining reliable real-time time behavior during power disruptions. To address these challenges, CARTOS introduces a mixed-preemption scheduling model that classifies tasks into computational and peripheral tasks, and ensures their efficient and timely execution by adopting just-in-time checkpointing for divisible computation tasks and uninterrupted execution for indivisible peripheral tasks. CARTOS also supports processing chains of tasks with precedence constraints and adapts its scheduling in response to environmental changes to offer continuous execution under diverse conditions. CARTOS is implemented with new APIs and components added to FreeRTOS but is designed for portability to other embedded RTOSs. Through real hardware experiments and simulations, CARTOS exhibits superior performance over state-of-the-art methods, demonstrating that it can serve as a practical platform for developing resilient, real-time sensing applications on IPDs.

## I. INTRODUCTION

Batteryless systems, often called intermittently-powered devices (IPDs), have the potential to revolutionize a variety of applications in Internet-of-Things (IoT), such as smart healthcare, agriculture, and building monitoring, where the use of batteries is undesirable or incurs significant maintenance costs. These systems harvest energy from ambient sources such as sunlight, heat, and radio signals, charge a small energy buffer, and execute intermittently for a short period of time whenever the energy is available. Since no batteries are needed, they have a much longer lifespan than battery-powered systems and can be deployed in harsh environments where batteries cannot operate properly, e.g., due to cold and hot temperatures [1]–[3]. This can also bring other benefits to system design such as smaller form factors and reduced manufacturing costs.

The aforementioned benefits, however, come with several technical challenges. First, given the variability in energy availability from ambient sources, IPDs must ensure the forward progress of program execution across power failures.

One of the most effective strategies is checkpointing [4]–[7], a method that involves inserting additional code snippets to store the state of a running program in non-volatile memory (NVM). When power is restored, the system can recover from the latest stored state, ensuring continuous progress. However, such static checkpointing introduces a high overhead and can significantly impact the performance of intermittent systems compared to conventional battery-powered embedded systems. Just-In-Time (JIT) checkpointing [8]–[10] mitigates this issue by making checkpoints dynamically only when the power goes low. However, it is difficult to be used for tasks with peripheral operations, e.g., sensor access and flash writing, because they cannot be paused and resumed at an arbitrary point, i.e., execution needs to be done atomically.

Secondly, IPDs should provide accurate time behavior even in the presence of intermittent power disruptions. This is particularly important for periodic sensing applications, which are one of the most in-demand areas of IoT. While many battery-powered IoT devices have been developed using conventional real-time operating systems (RTOS) for microcontrollers, such as FreeRTOS [11],  $\mu C/OS$  [12], RTEMS [13], to implement timely operations, they cannot offer forward progress guarantees in IPDs. For instance, a power failure during the execution of a sensor-reading or data-logging task can result in incomplete task execution or the loss or corruption of data. Therefore, it is crucial for the RTOS to consider the power consumption of tasks and the energy availability of the system. Furthermore, providing analytical support to understand how these devices will operate under diverse real-world circumstances is of great importance.

In this paper, we propose CARTOS, a charging-aware real-time operating system, as a practical platform to develop energy-resilient and reliable real-time sensing applications on IPDs. To achieve forward progress guarantees without losing efficiency, CARTOS classifies tasks into two types, computation tasks and peripheral tasks, and introduces a mixed-preemption scheduling model. Computation tasks are suspendable and resumable at any point of execution; hence, CARTOS schedules them preemptively and uses JIT checkpointing to store their states. On the other hand, since peripheral tasks are not JIT-checkpointable, CARTOS checks before their execution if the system has enough energy to complete them, and it schedules them non-preemptively to prevent interruption. Upon this model, CARTOS supports processing chains of tasks, i.e., tasks within an application have precedence constraints, which is common in practical sensing applications. CARTOS also adapts task scheduling based on environmental changes and ensures correct and timely execution under

This work is supported in part by grants from IITP (2021-0-00360), NSF (1943265), and USDA/NIFA (2020-51181-32198).

M. Karimi, Y. Wang, and H. Kim are with the Department of Electrical and Computer Engineering, the University of California Riverside, Riverside, CA 92521, USA (email: mkari007@ucr.edu; ywang665@ucr.edu; hyoseung@ucr.edu). Y. Kim and Y. Lim are with the Electronics and Telecommunications Research Institute, Daejeon 34129, South Korea (email: yb.kim@etri.re.kr; yoojin.lim@etri.re.kr).

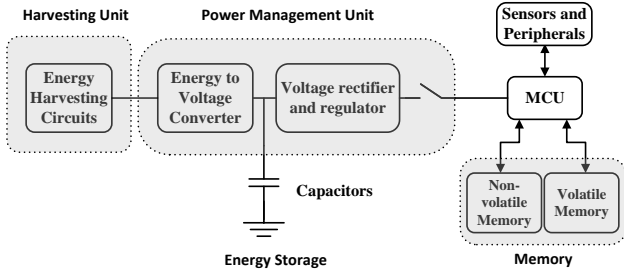


Fig. 1: A typical hardware design of IPDs

various conditions. Based on our system design, we provide analysis to test the timing behavior of processing chains of computation and peripheral tasks before deployment.

CARTOS is implemented by introducing new APIs and components to FreeRTOS, which is one of the most widely used embedded RTOS in real-world applications such as Amazon AWS IoT. However, as the design of CARTOS is not specific to FreeRTOS, it is portable to other RTOS as well. From our experiments on real hardware and simulation, CARTOS demonstrated several advantages over the state-of-the-art methods.

Section II provides an overview of previous work and establishes essential background information. In Section III, we introduce the proposed framework. Section IV presents the system model, the proposed mixed-preemption scheduling approach, and offers a detailed scheduling analysis. Section V presents the results of our evaluation. Lastly, Section VI summarizes and concludes this paper.

## II. BACKGROUND AND RELATED WORK

In this section, we give detailed background on IPD hardware characteristics and discuss state-of-the-art methods developed in the literature. We also review other studies related to energy-harvesting and IPD-based applications.

### A. IPD Hardware and Operation Phases

A typical hardware design of IPDs is illustrated in Fig. 1. The harvesting unit collects energy from the surrounding environment. It could be a solar cell, RFID receiver, or piezoelectric transducer. The power management unit (PMU) is responsible for converting and regulating the energy harvested by the energy harvester into a stable voltage that can be used to power the device's components. It also manages the device's power consumption to ensure that it does not exceed the available energy. Energy storage is usually a supercapacitor and is responsible for storing the collected electrical energy so that it can be used later when it is needed. The micro-controller unit (MCU) executes the device's software instructions and controls the device's various components. Memory stores the program code and data that the MCU uses to operate the device. Most IPDs have at least two types of memory: (i) volatile main memory equipped as part of MCU, e.g., SRAM, and (ii) nonvolatile memory to store execution progress during power loss, e.g., FRAM and MRAM. IPDs also often include sensors and peripherals, such as temperature, humidity, light sensors and wireless Bluetooth communication modules, to

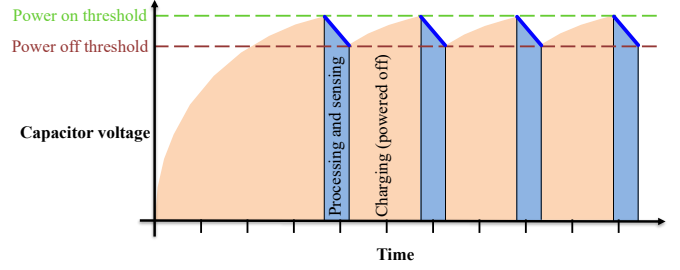


Fig. 2: Charging and discharging cycles of an IPD

monitor the device's environment, perform certain actions, and report any findings to the user.

The operation of an IPD can be broken down into the following three phases:

- 1) **Power-Off Phase:** In this initial phase, the device remains entirely powered off. It actively collects energy from the environment using an energy harvester and subsequently stores the gathered energy in a capacitor.
- 2) **Operation Phase:** Once the capacitor attains a sufficient voltage level, the PMU provides a consistent voltage supply to the device. This, in turn, enables the MCU to execute processing tasks and capture sensor data. The device continues in this phase until it reaches the predefined *power-off* threshold (going back to the power-off phase) or *low-voltage* threshold (moving on to the standby phase discussed next) depending on the design. Many prior IPDs [4], [14], [15] use only the power-off threshold for simplicity and they operate as in Fig. 2. The MCU starts processing and sensing activities when the capacitor voltage reaches a specific power-on threshold, and it continues until the voltage remains above the power-off threshold, at which point the device powers off. It is worth noting that charging can still happen while the system actively runs tasks in the operation phase; however, as the discharging rate is typically much higher than the charging rate, the capacitor voltage goes down over time.
- 3) **Standby Phase:** In this phase, energy-intensive components like the MCU, sensors, and radio units are either powered down or transitioned into sleep mode. Only the timekeeping ability, e.g., MCU's clock unit in low-power mode or external programmable RTC, remains active as it plays a crucial role in maintaining the precise time behavior of tasks [16]–[19]. The device remains in this state until the capacitor accumulates enough charge to return to the operation phase. This approach can be particularly useful in situations where the energy-harvesting rate is sporadic, as it allows the device to conserve energy and maintain the notion of time during periods of low power availability.

### B. Forward Progress Mechanisms

There has been extensive research on checkpointing to ensure that programs running on IPDs make forward progress and maintain data consistency across power failures. Static checkpointing [4]–[6], [20]–[22] inserts checkpointing code at the fixed locations of the program, which are determined

TABLE I: Comparison of previous work

Methods	JIT checkpointing	Peripherals	Long computations	Real-time scheduling	Energy adaptive	Analysis
Mementos [6]	✗	✗	✓	✗	✓	✗
Chinchilla [4]	✗	✗	✓	✗	✓	✗
Capybara [24]	✗	✓	✗	✗	✗	✗
Quickrecall [8]	✓	✗	✓	✗	✗	✗
Samoyed [10]	✓	✓	✓	✗	✓	✗
InK [23]	✗	✗	✗	✓	✓	✗
CatNap [9]	✓	✓	✓	✗	✓	✗
Celebi [17]	✗	✗	✓	✓	✓	✗
Rtag [16]	✗	✓	✗	✓	✗	✓
Karimi et al. [27]	✗	✓	✗	✓	✓	✓
CARTOS (this work)	✓	✓	✓	✓	✓	✓

by either the compiler support or manual programmer efforts. When a checkpoint is reached, the system saves the program’s state and relevant data to non-volatile storage, allowing the program to restart from that point in case of a power failure. Instead of finding checkpoint locations after writing the program code, new programming models have been studied to create checkpoints as part of the program’s execution flow [6], [7], [14], [15], [23]–[25]. In such models, the programmer needs to decompose a program logic into a collection of idempotent, atomic blocks with explicit input and output data.<sup>1</sup> Then, the input and output data of each task are recorded in NVM, which serves as checkpoints, e.g., data channels between tasks [7], [14]. However, this adds a significant burden to programmers to restructure their programs, which is particularly difficult for long-running computations, e.g., algorithm logic. In addition, programmers have to make sure that each atomic block is small enough to run within one charging cycle.

Just-In-Time (JIT) checkpointing [8]–[10], [26], on the other hand, makes checkpoints at runtime by capturing the current state of the system, including MCU register values and volatile data. To do so, the system needs to monitor the remaining energy and initiate JIT checkpointing when the low-voltage threshold is reached. This can bring performance benefits over static checkpointing by reducing the frequency of checkpointing and simplifying the programming of long-running computations [8], [26]. However, since peripheral operations cannot resume after reboot by recovering just the MCU’s state, JIT checkpointing cannot be used for them [10].

### C. IPD Task Scheduling

Task scheduling for batteryless devices can be categorized into two main types: *real-time* and *reactive* scheduling. Real-time scheduling focuses on executing periodic tasks with predictable charging behavior. These approaches aim to meet the deadlines of a specific set of tasks by assuming a certain amount of energy supply [16], [17], [27]. By doing so, they can guarantee tasks to be scheduled in a predictable manner and achieve consistent performance as long as the assumed energy model holds. On the other hand, reactive scheduling focuses on minimizing the overall response times of event-driven tasks [9], [23]. It starts task execution when the device’s energy reaches the predefined power-on threshold and stops when it drops below the power-off threshold. These approaches are

usually more flexible and may perform better with changing environmental conditions than the real-time approaches, but cannot ensure predictability and consistent performance due to their best-effort nature.

### D. Related Work

Table I presents a comprehensive comparison of various methods designed to address task execution on IPDs. As we already characterized prior work by category, we will discuss specific details of some of the work and additional related work below.

Among static checkpointing approaches, Mementos [6] proposes a method to automatically insert checkpointing code to the program at compile time. To reduce the cost of checkpointing, it also proposes to estimate the remaining energy and perform checkpointing only when the energy goes below a certain threshold. Chinchilla [4] also takes a similar approach. Capybara [24] relies on the programming model support for forward progress, and introduces a hardware-software co-design solution that includes a set of capacitors to handle tasks with different energy requirements.

Quickrecall [8] is a JIT checkpointing system but does not consider peripheral tasks. Samoyed [10] addresses this issue by introducing the *undo-logging* mechanism, which basically adds static checkpoints for peripheral operations. However, this approach is applicable only to the peripherals that “do not have internal non-volatile state and are arbitrarily restartable” [10] because of the idempotency requirement.

For real-time scheduling on IPDs, Celebi [17] proposes a scheduler that optimizes task scheduling based on known charging patterns. However, this method is primarily designed for independent computational tasks and may not handle peripheral tasks correctly because the scheduler does not ensure the atomicity and idempotency of task execution, e.g., the scheduler can stop a task at an arbitrary point. Karimi et al. [16] introduce a real-time scheduler designed to atomically execute independent periodic tasks with various energy requirements and provide a formal analysis of task schedulability for a fixed charging rate of the system. The same authors [27] present an energy-adaptive scheduler to minimize the age of information. While these approaches contribute to enabling real-time operations on IPDs, none of them are sufficient to handle real-world applications that consist of a chain of peripheral access and long-running computations.

There are also other previous studies that focus on running neural networks on IPDs [18], [28], enabling multiple

<sup>1</sup>They call such atomic blocks *tasks* in their work, but we avoid using their term since tasks in our paper refer to threads in conventional RTOS.

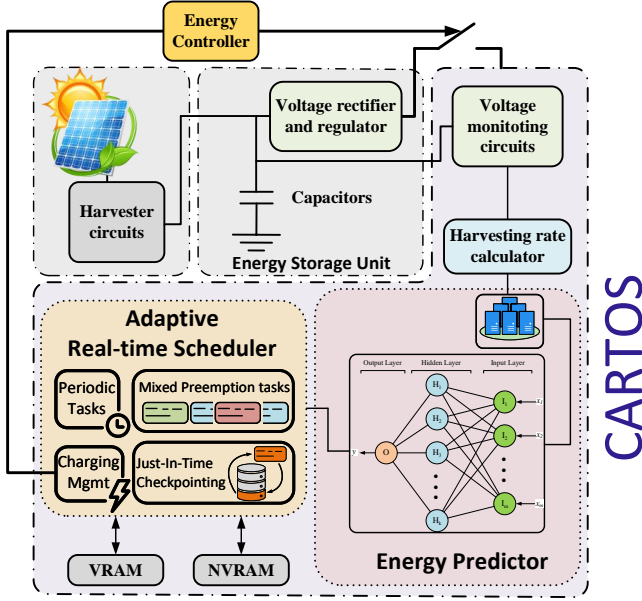


Fig. 3: System Framework

energy buffers [29], energy-aware memory mapping [30], communication on IPDs [31], and zero-power timekeeping methods [32]. They contribute to expanding the application scope of IPDs and our work does not conflict with them.

### III. CARTOS FRAMEWORK

This section presents our proposed CARTOS framework. Fig. 3 depicts the overview of the framework. CARTOS targets typical IPD hardware as discussed in Sec. V-A (left upper corner of the figure) and introduces additional circuitry to monitor and control the power of the entire board (right upper corner). CARTOS includes an adaptive real-time scheduler that is built upon our mixed-preemption scheduling model to support applications with a chain of peripheral and long-running computational tasks. CARTOS also includes a neural network-based energy (charging rate) predictor to adapt to changing environmental conditions. In the rest of this section, we will first describe the hardware setup for CARTOS and then present the major software components of our framework.

#### A. Hardware Setup

CARTOS targets an IPD that is equipped with an MCU capable of running a conventional RTOS such as FreeRTOS. The IPD is expected to have both volatile memory (SRAM) and non-volatile memory (NVM). Although we used an ARM Cortex-M4 MCU in our implementation, there is no other restriction imposed on MCUs by CARTOS.

While different energy sources can be used, we primarily consider solar energy as a harvesting source. Hence, we assume the IPD has a solar harvesting unit that collects energy from the sun and converts it into usable electrical energy. The harvested energy is then stored in a capacitor to drive the IPD.

In order to utilize all three operational phases discussed in Sec. II-A and support our scheduling behavior, CARTOS assumes that IPD hardware provides the ability to (i) monitor the current charging rate and the remaining energy level of the

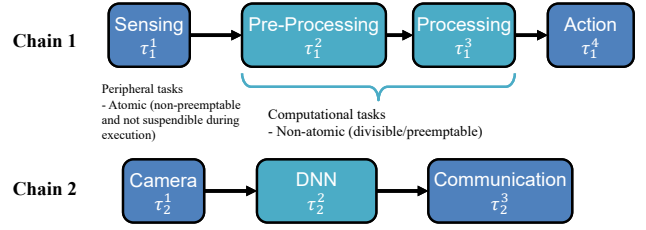


Fig. 4: An example of multiple chains with different tasks

capacitor, and (ii) cut off power supply to the processing part of the board, e.g., MCU, NVM, sensors, etc., for a requested interval. Item (i) is the voltage monitoring circuits and item (ii) is the energy controller in Fig. 3. Those can be integrated with other hardware components on the same board or can be realized in a separate board, as we did in our implementation (see Sec. V-A).

#### B. Task Chains and Mixed Preemption Model

CARTOS supports periodic applications that consist of a processing chain of tasks, which is a common design pattern found in sensing and intelligent applications [14], [33]–[36]. Fig 4 illustrates two processing chains, one comprising four tasks and the other with three tasks. Each task  $\tau_i^j$  on a chain  $i$  can be either a peripheral or computation task.<sup>2</sup> The chain can start execution when its first task is released (e.g., the periodic sensing task  $\tau_1^1$  on chain 1) and the subsequent tasks are eligible to run only when their preceding task finishes (e.g., the action task  $\tau_1^4$  becomes “ready” after the completion of the processing task  $\tau_1^3$ ). We assume that the first task of a chain is a periodic task, triggered by either a timer or an external event. Hence, all other tasks of the same chain follow the same periodic pattern with precedence constraints among them.

1) *Mixed-Preemption Model*: Recall that processing chains can consist of a mixture of peripheral and computation tasks. Peripheral tasks need to be executed *atomically*, especially when the corresponding hardware maintains internal state [10]. To ensure the atomic execution of peripheral tasks, CARTOS schedules peripheral tasks non-preemptively, i.e., once selected for scheduling, it will continue with no preemption from other higher-priority tasks. However, this is not enough for atomicity. The adaptive scheduler of CARTOS (Sec. III-C) waits until enough energy is charged to complete the execution of a peripheral task for this period before scheduling that task. This guarantees that the system does not turn off at least until the completion of the peripheral task, thereby achieving correctness. On the other hand, computational tasks are scheduled preemptively, just like other RTOS, and CARTOS manages their forward progress by JIT checkpointing. To summarize, peripheral and computational tasks in CARTOS have the following characteristics:

- Peripheral tasks: atomic, non-preemptable (i.e., not suspendable while it is actively executing; unable to JIT checkpoint)
- Computational tasks: non-atomic, preemptable (i.e., suspendable at any time; can be JIT checkpointed)

<sup>2</sup>Detailed chain and task parameters needed for analysis will be provided in Sec. IV.



This mixed-preemption model is the basis for our scheduler presented in the next section. The type of a task (atomic or non-atomic) is configurable when the user creates a task. For ease of presentation, we will use peripheral and atomic tasks interchangeably. The same applies to computational and non-atomic tasks.

```
void TaskRunner(void const * argument)
{
    /* Set the task's period and offset to 10 and 2
       seconds, respectively */
    setTaskPeriod(10000, 2000);

    while (1)
    {
        /* Body of the task */
        printf("Task one is scheduled!\r\n");

        /* Suspends the task until next period is reached */
        waitForNextPeriod();
    }
}
```

Fig. 5: Periodic task example in CARTOS

2) *Support for Periodic Tasks and Chains*: CARTOS offers APIs to assist the programming and execution of periodic tasks. Users can define tasks as periodic and specify their required periods and release offset based on the application's demands. Specifically, the APIs are:

- `setTaskPeriod(period, offset)`: This makes the calling task run periodically after the given initial release offset. The second parameter is optional.
- `waitForNextPeriod()`: This tells the kernel that the calling task has finished its execution for the current period. The task will be suspended immediately and will be released (ready state) at the start of the next period.

Fig. 5 depicts the example of a periodic task (`taskRunner`) in CARTOS. `setTaskPeriod()` is called at the beginning of the task's code, declaring that it is a periodic task. The task has a while-loop where each iteration represents a job for each period. When the task reaches the end of execution in the current period, it calls `waitForNextPeriod()`. Then, the scheduler removes it from the ready queue and sets the system timer to insert the task back to the ready queue at the start of the next period.

For chained task execution, CARTOS also allows the user to create chain objects in the kernel and assign periodic tasks to specific chains. While chain objects are not schedulable entities, they help control the execution order of tasks within a chain. Once tasks are assigned to a chain, these tasks are removed from the ready queue and made inactive. Chain execution commences with the release of the first task, which is triggered by either a timer or an external event as we explained earlier. When the first task finishes its job through the invocation of `waitForNextPeriod()`, the subsequent task in the chain is set ready and becomes eligible for execution by the scheduler. This continues until the last task of the chain. Consequently, if all tasks within the chain can complete execution within one chain period (equivalent to the period of the first task), only one task from the chain is ready at any given time. This approach enforces the precedence

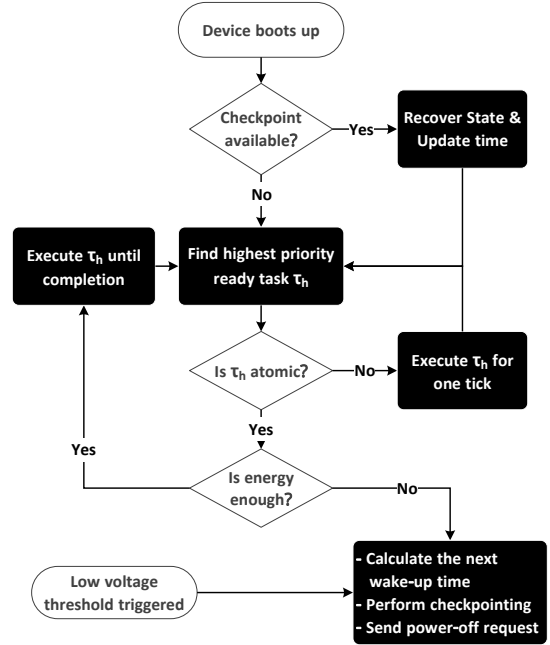


Fig. 6: Scheduler operation flowchart

constraints within a chain while allowing our scheduler to follow the task-level priority-based scheduling policy.

### C. Adaptive Real-Time Scheduler

The real-time scheduler of CARTOS is designed to utilize efficiently available energy while supporting both peripheral (atomic) and computational (non-atomic) tasks. In doing so, it prioritizes the execution of higher-priority tasks that are ready over those with lower priority, a crucial feature for RTOS to meet timing requirements. By adhering to the priority-based scheduling policy, CARTOS minimizes the risk of missing important deadlines, thereby enhancing the system's overall performance and reliability.

Fig 6 illustrates the operation flow of the scheduler from the device boot-up. Upon boot-up, the scheduler checks for the presence of any valid JIT checkpoint in NVM. If a checkpoint is found, the device restores tasks from this checkpoint and updates the system time and timer events, including those of `waitForNextPeriod()` from periodic tasks.

For scheduling tasks, the scheduler first finds the highest-priority task  $\tau_h$  from the ready queue. It is worth noting that the scheduler does not need to consider the execution order of tasks within chains here, because such precedence constraints are controlled by the chain support explained in the previous section. Then, the scheduler checks if the highest-priority task  $\tau_h$  is atomic (peripheral) or not and the scheduling behavior changes according to the task type.

If the task  $\tau_h$  is non-atomic (computational), the scheduler executes  $\tau_h$  for one tick of time (scheduling time quantum; 1 ms in our implementation) and repeats the above procedure to find the highest-priority ready task again for preemptiveness. Note that this is the case for tick-based RTOS. In the case of a tickless system,  $\tau_h$  can continue to run until it voluntarily relinquishes the CPU or any higher-priority task than  $\tau_h$  becomes ready.

If  $\tau_h$  is atomic (peripheral), the scheduler checks the required energy for  $\tau_h$ 's job execution based on the profiled data, and compares it with the current system energy level, measured through the voltage level of the capacitor (more details on this will be given in the next subsection). If the system's available energy is higher than the amount required to ensure the uninterrupted execution of the given atomic task, the scheduler dispatches this task and the task will continue until its job is completed, i.e., non-preemptive execution. Otherwise, it proactively enforces a power cycle to harvest more energy.<sup>3</sup> In doing so, it first estimates the *required harvesting time*,  $\Delta t$ , considering the predicted charging rate and the current voltage level, and then computes the *next device wake-up time* from the standby phase by taking into account both the estimated harvesting time and the future release times of other higher-priority periodic tasks. This is done to ensure that higher-priority tasks are not missed during charging. For example, if a high-priority task  $\tau_1$  needs to be released at time  $t_1$  while the device is being charged for a low-priority task  $\tau_2$ , the charging process should be stopped so that the high-priority task  $\tau_1$  is scheduled. Therefore, the next wake-up time from the standby phase is obtained by taking the minimum between the required harvesting time and the earliest future release time of higher-priority tasks than  $\tau_h$ . Subsequently, the device is powered down (after necessary JIT checkpoint operations), and the atomic task  $\tau_h$  as well as other tasks are scheduled when the device is powered on. It should be noted that such a proactive power-cycling sequence happens before reaching the low-voltage threshold. When the device reaches a low-voltage threshold, the device power cycling is managed by the JIT checkpointing service presented next.

#### D. JIT Checkpointing Service

In CARTOS, JIT checkpointing is implemented as a system service task. This service monitors if the capacitor voltage level reaches the low-voltage threshold, which can be implemented as an external interrupt or periodic polling of the voltage monitoring circuits. The JIT service task is launched as part of the boot-up sequence and executes with the highest priority in the system to execute as soon as possible when needed.

The low-voltage threshold can be triggered at any time during non-atomic preemptive task execution (recall that our scheduler executes atomic tasks only when the device has sufficient energy to complete their jobs). Then, the JIT service task enforces a new power cycle in a similar procedure as stated before. Specifically, it is in charge of performing JIT checkpointing operations. It iterates over all non-atomic tasks in the system, and for each non-atomic task, it stores the task's context (task control block), stack, and SRAM data areas to NVM so that those can be restored to SRAM upon the next power-on. The JIT service also stores the current system time and timer events in NVM in order to ensure the correct execution of timer-based operations across power cycles. Once

the device powers up, the boot-up procedure restores non-atomic tasks and updates the system time and timer events. The time update can be done in two ways. If there is an external RTC, e.g., as part of the energy controller, it can simply update the system time based on it. Otherwise, it can estimate the current time by adding the latest checkpointed system time and the power-up time that was computed before power cycling (Sec. III-C and Fig. 6). We use the latter approach in our implementation.

#### E. Charging Management

While JIT checkpointing facilitates the proper execution of non-atomic tasks, charging management is vital to ensure the execution of atomic tasks. To address this, we assign a voltage threshold  $V_i^j$  to each atomic task  $\tau_i^j$ . This threshold represents the minimum voltage that the system requires before starting the execution of task  $\tau_i^j$ 's job, thereby ensuring that the task can be completed before reaching the low-voltage threshold used for JIT checkpointing. The calculation for  $V_i^j$  is as follows:

$$V_i^j = \sqrt{\frac{2Q_i^j W_S + \mathbb{C} V_{min}^2}{\mathbb{C}}} \quad (1)$$

where

- $C_i^j$ : Worst-case execution time of a job of the task  $\tau_i^j$
- $Q_i^j$ : Charging time of the task, which is the amount of time required to charge to perform  $C_i^j$  of execution.
- $W_S$ : Energy-harvesting rate of the system
- $\mathbb{C}$ : Capacitor size in Farad
- $V_{min}$ : Low-voltage threshold that triggers JIT checkpointing and power cycling

Eq. (1) is derived from the well-known calculation on the energy changes in a capacitor when it receives a fixed power of  $W$  from time  $t_1$  to  $t_2$ , given by

$$\Delta E = \frac{1}{2} \mathbb{C} (V_2^2 - V_1^2) = W (t_2 - t_1) \quad (2)$$

To derive Eq. (1) from the above equation,  $(t_2 - t_1)$  is substituted with  $Q_i^j$ ,  $W$  is substituted with  $W_S$ ,  $V_2$  is substituted with  $V_i^j$ , and  $V_1$  is substituted with  $V_{min}$ .

In Eq. (1), the values of  $C_i^j$  and  $Q_i^j$  are specific to each task, while  $V_{min}$  and  $\mathbb{C}$  are the system parameters given by the user at design time. The charging rate of the system,  $W_S$ , is updated at runtime using an energy predictor as the environment changes. Additionally, after each job execution, the value of the worst-case execution time  $C_i^j$  is profiled and updated in the task's task control block (TCB). If there is a change in  $C_i^j$  or  $W_S$ , the value of  $Q_i^j$  for that task is also updated at runtime. The calculation for updating  $Q_i^j$  is as follows:

$$Q_i^j = \frac{(W_i^j - W_S) \times C_i^j}{W_S} \quad (3)$$

where  $W_i^j$  is the discharging rate of  $\tau_i^j$ .

When scheduling an atomic task  $\tau_i^j$ , the scheduler compares current voltage level of the system,  $V_{current}$ , with  $V_i^j$ . If the current voltage level exceeds  $V_i^j$ , then the scheduler starts executing the task until its completion. Otherwise, the required

<sup>3</sup>Precisely speaking, the device transitions to the standby phase using the energy controller unit discussed in Sec. III-A.

harvesting time  $\Delta t$  is calculated by the following equation and a power cycle is scheduled:

$$\Delta t = \frac{\mathbb{C} \left( V_i^{j^2} - V_{current}^2 \right)}{2 \cdot W_S} \quad (4)$$

The energy harvesting rate,  $W_S$ , can change over time depending on environmental conditions. As the required harvesting time and the next device wake-up time rely on this, it is crucial to obtain a precise value of  $W_S$  for efficient operations because the over-estimation makes the device turn on unnecessarily late and the under-estimation lets the device turn on and off multiple times until it reaches the required charge level. To address this issue, CARTOS employs a machine learning-based energy prediction model proposed in [27]. This model is a simple yet viable approach for MCU-level devices, providing a reliable prediction of solar harvesting rates by leveraging the temporal dependencies of time-series voltage data. In our implementation, we integrated this model into CARTOS and used a 30-minute interval for our prediction window.

#### IV. MIXED-PREEMPTION PROCESSING CHAIN ANALYSIS

This section gives a schedulability analysis of processing chains running in CARTOS. The ability to check if chains will be able to meet their deadlines is important since such information can be used to predict the performance of the system before deployment and provides an opportunity to further optimize hardware and software designs. In the following, we describe the system model and assumptions made for analysis purposes and provide our analysis for chains of tasks.

##### A. System Model

We consider a system with  $n$  processing chains. A chain  $i$  is modeled as  $\Gamma_i : (C_i, T_i, D_i, Q_i)$ , where  $C_i$ ,  $T_i$ , and  $D_i$  are the worst-case execution time, period, deadline, and charging time of one instance (job) of the chain. Each chain  $\Gamma_i$  is comprised of  $m_i$  tasks. Each task is either atomic (non-preemptable) or non-atomic (preemptable), following the mixed-preemption model of CARTOS. A task  $j$  of a chain  $\Gamma_i$  is denoted as  $\tau_i^j : (C_i^j, T_i^j, D_i^j, Q_i^j)$ , where  $\forall j \leq m_i \mid T_i^j = T_i, C_i = \sum_{j=1}^{m_i} C_i^j, Q_i = \sum_{j=1}^{m_i} Q_i^j$ , i.e., all the tasks within the same chain share the same period as their chain and the execution time of the chain is the sum of the execution of all tasks in that chain. Tasks in a processing chain are ordered in sequence. Hence, for a processing chain to complete, all of its tasks should complete their execution in that order, i.e.  $\tau_i^1$  should be the first task to be executed and then  $\tau_i^2$  and so on.

Each chain  $\Gamma_i$  has a priority of  $\pi_i$ , e.g.,  $\pi_h > \pi_i$  means  $\Gamma_h$  is a higher-priority chain than  $\Gamma_i$ . Tasks within a chain share the same task-level priority and they are executed in order.

We use  $R_i$  to denote the worst-case response time of a chain  $\Gamma_i$ . A system with  $n$  processing chains is said to be *schedulable* when the response times of all the chains are smaller than or equal to their deadlines, i.e.,  $\forall i \leq n \mid R_i \leq D_i$ .

In real-world scenarios, the energy harvesting rate of the system and the charging time of tasks can vary with the availability of energy resources. However, especially for the solar energy we consider in this work, the changes are relatively

slow (e.g., over several tens minutes and hours) and do not typically happen within a chain period or the hyperperiod of chains. Therefore, a fixed energy harvesting rate is considered for analysis purposes while our runtime system can still adapt to such changes.

##### B. Schedulability Analysis

Recall our mixed-preemption scheduling model. Atomic tasks are non-preemptibly scheduled, so once started, they cannot be preempted by any other tasks. On the other hand, non-atomic tasks are preemptable by higher-priority tasks during their execution. To analyze the worst-case response time of a chain comprised of such tasks, we extend two existing methods: the task-level mixed preemption analysis without energy constraint [37], and the non-preemptive IPD task scheduling analysis [16], both of which are exact analysis. Our extension takes into account the charging requirements of tasks and the execution order within chains, as follows.

The level- $i$  active period plays an important role in computing the worst-case response time when non-preemptiveness is involved. As such, we first revise the existing calculation of the level- $i$  active period for a task to our processing chain model. The level- $i$  active period of a chain  $\Gamma_i$  with the charging time  $Q_i$  can be computed recurrently by:

$$L_i^{(s)} = B_i + \sum_{h: \pi_h < \pi_i} \left\lceil \frac{L_i^{(s-1)}}{T_h} \right\rceil (C_h + Q_h) \quad (5)$$

where  $B_i$  is the blocking time due to a non-preemptive task from a lower-priority chain and  $Q_h$  is the charging time of  $\Gamma_h$ .  $B_i$  can be obtained by

$$B_i = \max_{\forall l, j \mid \pi_l < \pi_i \wedge A_l^j = \text{true}} \{C_l^j\} \quad (6)$$

where  $A_l^j$  indicates the atomicity of a task  $\tau_l^j$ , i.e.,  $A_l^j = \text{true}$  if  $\tau_l^j$  is atomic (non-preemptable) and  $A_l^j = \text{false}$  if  $\tau_l^j$  is non-atomic (preemptable). The iteration of Eq. (5) starts with  $L_i^{(0)} = B_i + C_i$  and stops when  $L_i^{(s)} = L_i^{(s-1)}$  (converged) or  $L_i^{(s)} \geq T_H$  where  $T_H$  is the hyperperiod of all chains in the system (failed). Here, the charging time  $Q_h$  is added to the execution time  $C_h$  because CARTOS can effectively delay execution by up to this amount when the charge is insufficient (recall our scheduler and JIT checkpointing service in Sec. III).

The use of the level- $i$  active period,  $L_i$ , allows us to find the worst-case response time of a chain  $\Gamma_i$  by considering the response times of all jobs of  $\Gamma_i$  within  $L_i$ . Specifically, the chain response time  $R_i$  can be obtained by

$$R_i = \max_{k \leq K_i} \{F_{i,k} - (k-1)T_i\} \quad (7)$$

where  $K_i$  is the number of jobs of  $\Gamma_i$  within  $L_i$ , i.e.,  $K_i = \left\lceil \frac{L_i}{T_i} \right\rceil$ , and  $F_{i,k}$  is the finishing time of the  $k^{\text{th}}$  job of  $\Gamma_i$  in  $L_i$ . Since tasks within a chain are executed sequentially,  $F_{i,k}$  is equal to the finishing time of the last task  $\tau_{i,k}^{m_i}$  of  $\Gamma_i$ , i.e.,

$$F_{i,k} = F_{i,k}^{m_i} \quad (8)$$

If the last task  $\tau_{i,k}^{m_i}$  is atomic, due to non-preemptiveness, its latest finishing time  $F_{i,k}^{m_i}$  is calculated by

$$F_{i,k} = S_{i,k}^{m_i} + C_i^{m_i} \quad (9)$$

where  $S_{i,k}^{m_i}$  is the start time of  $\tau_{i,k}^{m_i}$ 's execution and we discuss this later.

If the task  $\tau_{i,k}^{m_i}$  is non-atomic,  $F_{i,k}$  is obtained by the following recurrence, taking into account preemption caused by higher-priority chains during the start and finish time of the task  $\tau_{i,k}^{m_i}$ :

$$F_{i,k}^{(s)} = S_{i,k}^{m_i} + C_i^{m_i} + \sum_{h:\pi_h > \pi_i} \left( \left\lceil \frac{F_{i,k}^{(s-1)}}{T_h} \right\rceil - \left( \left\lfloor \frac{S_{i,k}^{m_i}}{T_h} \right\rfloor + 1 \right) \right) (C_h + Q_h) \quad (10)$$

The iteration in Eq. (10) can start with  $F_{i,k}^{(0)} = S_{i,k}^{m_i} + C_i^{m_i}$ .

To find the start time of task  $\tau_{i,k}^{m_i}$ ,  $S_{i,k}^{m_i}$ , we should consider the following factors: (i) blocking caused by lower priority chains, (ii) preemption caused by higher priority chains, (iii) execution time of previous jobs of the chain  $\Gamma_i$ , (iv) executions of all other tasks in the chain  $\Gamma_i$  that should be serviced before the task  $\tau_{i,k}^{m_i}$ , and (v) all the overheads caused by charging. Note that the job of the chain  $\Gamma_i$  can be blocked only once during its entire job execution due to the priority-based scheduling of CARTOS. Therefore, for the task  $\tau_{i,k}^{m_i}$ , the start time  $S_{i,k}^{m_i}$  can be computed by the following recurrence:

$$S_{i,k}^{m_i(s)} = B_i + (k-1)C_i + \sum_{p=1}^{m_i-1} C_i^p + \sum_{h:\pi_h > \pi_i} \left( \left\lceil \frac{S_{i,k}^{m_i(s-1)}}{T_h} \right\rceil + 1 \right) C_h + \nu_{i,k}^{(s)} \quad (11)$$

where the starting condition is

$$S_{i,k}^{m_i(0)} = (k-1) \cdot T_i + B_i + \sum_{p=1}^{m_i-1} C_i^p \quad (12)$$

In Eq. (11),  $\nu_{i,k}^{(s)}$  is the total amount of time required for  $k$  jobs of the chain  $\Gamma_i$  to acquire their own portions of charge. This can be calculated at each iteration by considering the charging time of higher-priority chain jobs:

$$\nu_{i,k}^{(s)} = k \times Q_i + \sum_{h:\pi_h > \pi_i} \left( \left\lceil \frac{S_{i,k}^{m_i(s-1)}}{T_h} \right\rceil + 1 \right) Q_h \quad (13)$$

From the above, we can compute the worst-case response time of each chain and test the schedulability of the system.

## V. EVALUATION

We first demonstrate the effectiveness of CARTOS by using our implementation on a real system. Then, we perform schedulability experiments to evaluate how well our scheduling framework performs compared to the state-of-the-art under various conditions.

### A. Hardware Setup

Fig. 7 depicts the hardware setup for our experiments. This includes a processing board equipped with an STM32L496ZG MCU (ARM Cortex-M4) and an external nonvolatile MRAM module. To supply power, we make use of an energy harvesting board comprising a 0.47F capacitor, LTC3588 energy

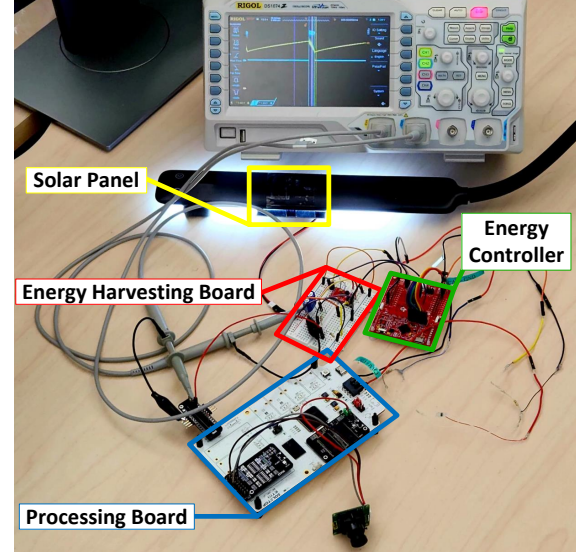


Fig. 7: The hardware setup for evaluation

harvester, and a 2W solar panel. Furthermore, an energy controller board featuring an ultra-low-power MPS430 MCU is used to control the power supply to the processing board. We have also integrated and configured a camera within the system to facilitate applications related to image processing. In our setup, the power-on and power-off thresholds are 4.8V and 3.8V, respectively. The low-voltage threshold is set to 4.0V and the difference between the power-off and low-voltage thresholds is to ensure enough energy for JIT checkpointing.

The processing board interacts with the energy controller board using serial communication. The interaction is mainly to request power cut-off for a given amount of time. To control the power connection between the energy harvesting board and the processing board, MOSFET transistors are used as a switch. This switch is placed between the regulated power from the energy harvesting board and the processing board and is controlled by the energy controller.

### B. Real System Experiments

We consider two experimental scenarios to demonstrate the performance of CARTOS against the standard JIT checkpointing method that allows preemptive scheduling and the state-of-the-art (SOTA) real-time IPD scheduler [16] that executes all tasks non-preemptively. In both methods, priority-based scheduling is used for fairness of comparison.

The first scenario is designed to evaluate the ability to handle peripheral tasks with long execution time. The system is configured to run two chains. The first chain contains three tasks running with high priority, where the first and last tasks are non-preemptable (peripheral) and the second task is preemptable (computational). The second chain has one non-preemptable task  $\tau_2$  with extended execution time and running with low priority. The task parameters are detailed in Table II.

Fig. 8a illustrates the execution behavior of tasks in the first scenario under the JIT checkpointing method. The release offset of all tasks is set to zero, resulting in all jobs arriving at time  $t = 0$ . After the execution of the first three high-priority jobs ( $\tau_1^1, \tau_1^2, \tau_1^3$ ), the execution of the chain 2 task



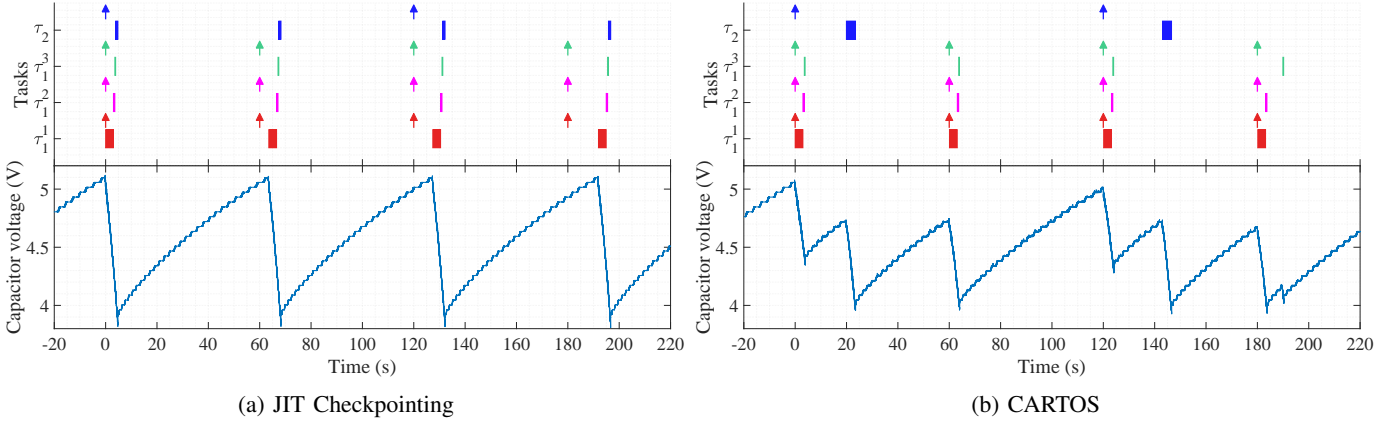


Fig. 8: Task execution behavior of the proposed method compared to JIT checkpointing

TABLE II: Task parameters for first scenario

	$C$ (ms)	$T$ (s)	$D$ (s)	$\pi$	Preemptable
$\tau_1^1$	3000	60	59.2	2	N
$\tau_1^2$	500	60	59.7	2	Y
$\tau_1^3$	300	60	60	2	N
$\tau_2$	3500	120	120	1	N

TABLE III: Task parameters for second scenario

	$C$ (ms)	$T$ (s)	$D$ (s)	$\pi$	Preemptable
$\tau_1$	3000	40	40	2	N
$\tau_2$	5000	200	200	1	Y

$\tau_2$ , starts. However, during the execution of  $\tau_2$ , the device's energy level drops to the low-voltage threshold, causing it to shut down the device. Upon the next boot-up, new jobs from high-priority tasks are released and subsequently executed. As  $\tau_2$  is a non-preemptive atomic task, it restarts its execution from the beginning, repeating the same execution pattern until  $\tau_2$  misses its deadline at  $t = 120$ s.

Conversely, as illustrated in Fig. 8b, CARTOS does not begin the execution of  $\tau_2$  when the first three jobs of high-priority tasks finish. Instead, it finds that the charging level is insufficient to complete  $\tau_2$ 's execution, and initiates power cycling just enough to charge the demand of  $\tau_2$ . Consequently, the device wakes up at  $t = 20$ s, and  $\tau_2$  executes successfully without interruption. These results show that JIT checkpointing lacks the ability to accommodate non-preemptable tasks and can lead to energy wastage.

The second scenario involves a long computational (pre-emptive) task. The system has two single-task chains: the high-priority chain  $\Gamma_1$  has a non-preemptive task  $\tau_1$  with a shorter execution time and the low-priority chain  $\Gamma_2$  has a preemptive task  $\tau_2$  with a longer execution time.  $\Gamma_1$  has a release offset of 10ms, while  $\Gamma_2$  has a release offset of zero. The task parameters are detailed in Table III.

Fig. 9a shows the results of the SOTA real-time IPD scheduler [16]. Due to the non-zero release offset of the high-priority task  $\tau_1$ , the low-priority task  $\tau_2$  starts first at  $t = 0$ . The non-preemptive scheduling behavior of [16] makes this task continue its execution until completion. At time 5 when  $\tau_2$  finishes, the device shuts down to accumulate enough energy to run  $\tau_1$ . This makes the first job of the high-priority task  $\tau_1$  complete its execution after  $t = 40$ s, resulting in a deadline miss and subsequently skipping its second job.

In the case of CARTOS, both tasks meet their deadlines as shown in Fig. 9b. Even though the low-priority task  $\tau_2$  begins execution at  $t = 0$ , it is soon preempted by the high-priority task  $\tau_1$ , allowing  $\tau_1$  to meet its deadline. The execution of the job of  $\tau_2$  spans across multiple power cycles and it finishes at around  $t = 163.5$ s, which is before its deadline. This result demonstrates the effectiveness of our mixed-preemption scheduling especially when long-running computational tasks are involved.

### C. Analytical Experiments

In this section, we compare the schedulability of the SOTA real-time IPD scheduler [16] and our work. The experiments are conducted in MATLAB on a workstation equipped with an Intel 4.2GHz Core i7 CPU with 16GB of RAM. Since the SOTA method does not support the analysis of processing chains, we only generated single-task chains for comparison. Therefore, we refer to the generated chains as tasks in the rest of this section.

To determine the execution time of each task for our experiments, we choose the period randomly from 1s to 60s, find the task's utilization using the UUniFast method [38], and then multiply this utilization by the task's period and round the result to the nearest positive value with one decimal point accuracy. In simpler terms, we determine the task execution time as  $C_i = \max(\lfloor 10 \cdot T_i \cdot U_i \rfloor / 10, 0.1)$ .

We begin by assessing the impact of discharging rates on schedulability. This experiment involves categorizing tasks into two distinct groups: those with high energy demands and those with low energy demands. For the high-energy demand tasks, the discharging rate is selected randomly from the range of 8 to 10, while for the low-energy demand tasks, it is chosen from 1 to 3. We introduce variations in the proportion of low-energy demand tasks, ranging from 0 to 100%. For each configuration of the low task demand ratio, we create 1000 tasksets and calculate the average schedulability rate across these sets. In this experiment, the number of tasks in a taskset is set to 5 and the utilization of the taskset is randomly selected from a range of 0.1 to 0.9. The atomicity of each task (i.e., if the task is preemptable or non-preemptable) is also selected randomly. The priorities of tasks for each taskset are assigned based on the Rate-Monotonic method (i.e., tasks with lower

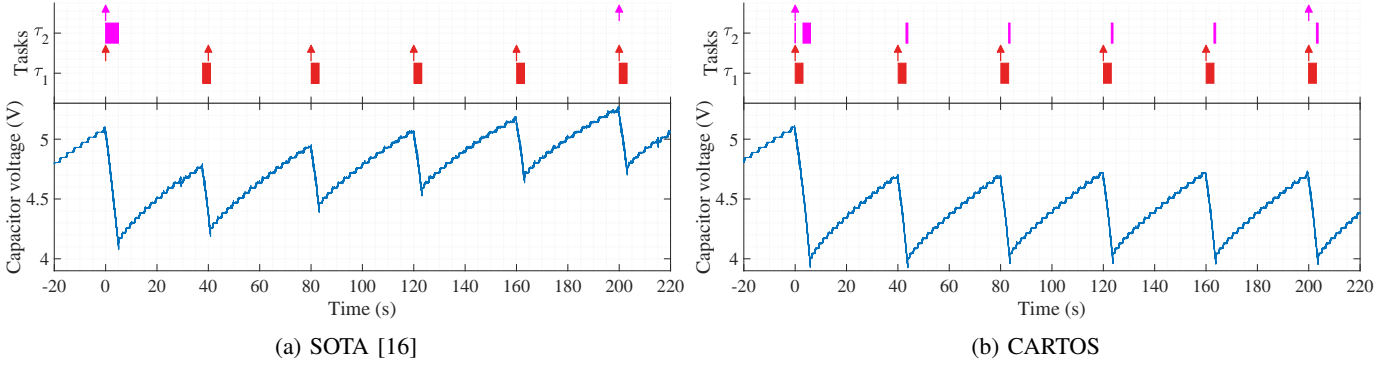


Fig. 9: Task execution behavior of the proposed method compared to the [16] method

periods get higher priority). The charging rate is fixed to 3, and implicit deadlines are considered, i.e.,  $D_i = T_i$ .

Fig. 10 shows that CARTOS outperforms SOTA by up to 20% of schedulability. This is mainly due to the unnecessary blocking time caused by lower-priority tasks in SOTA which treats all tasks non-preemptible even if some are fully computational tasks. The gap between the two methods increases with the number of low-energy demand tasks because the negative impact of the blocking time outweighs the energy constraint.

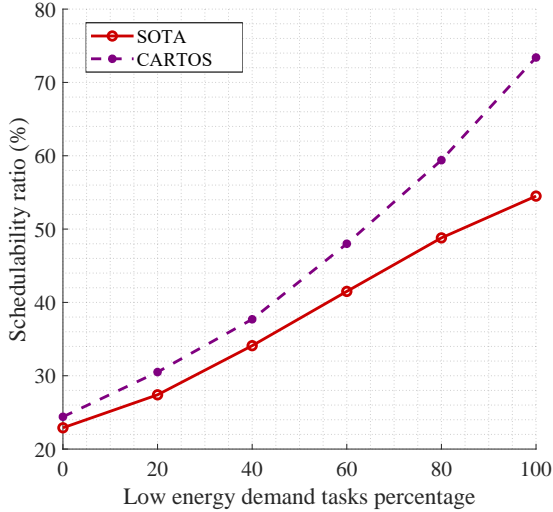


Fig. 10: Scheduler performance with various discharging rates

Next, we evaluate the impact of utilization on taskset schedulability. In this experiment, the taskset utilization is chosen from 0.1 to 0.9 with 0.1 steps. For each taskset utilization, 1000 tasksets are generated and the average schedulability ratio of the total 1000 tasksets is reported. The number of tasks, period, and discharging rate of each task are chosen randomly from 3 to 8, from 1s to 60s, and from 1 to 10, respectively. We use the same method as the previous experiment to calculate the execution time for each of the tasks within a taskset.

Fig. 11 shows the results. The schedulability improvement of CARTOS over SOTA tends to increase with the taskset utilization although the gap is smaller than in the previous experiment. From these results, we conclude that the energy constraint is indeed the major factor contributing to the schedulability performance in IPDs and the benefit of

our mixed-preemption approach will be tremendous when the system has long-running computational tasks along with peripheral tasks.

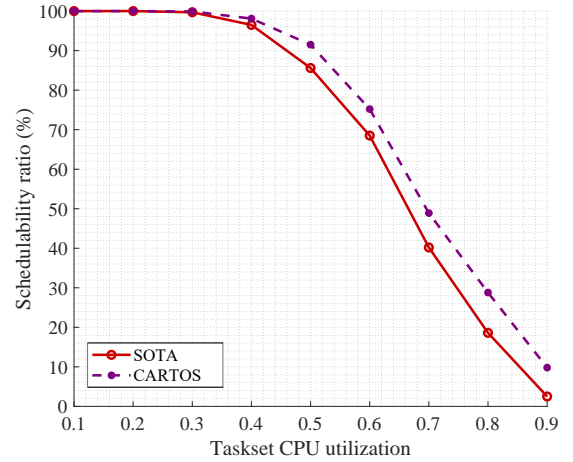


Fig. 11: Scheduler performance with various utilization rates

## VI. CONCLUSION

In this paper, we introduced CARTOS, a charging-aware real-time operating system for intermittently-powered battery-less devices. CARTOS leverages a mixed-preemption scheduling model to facilitate correct and efficient execution of periodic sensing applications, comprised of a chain of computational and peripheral tasks. For computational tasks, it schedules non-preemptively while ensuring forward progress through just-in-time (JIT) checkpointing. For peripheral tasks, it guarantees atomicity by scheduling them non-preemptively and charging sufficient energy to complete their jobs before execution. Furthermore, CARTOS includes energy management that computes the required charging time and utilizes a machine-learning-based energy predictor to update the harvesting rate to adapt to changing environmental conditions. We evaluated CARTOS through real system experiments as well as schedulability experiments. Our results showed that CARTOS can successfully schedule periodic chains of tasks, while state-of-the-art fails to do so. Furthermore, CARTOS outperformed state-of-the-art by up to 20% in schedulability across various experimental settings.

For future work, we plan to expand the capabilities of CARTOS to accommodate a more diverse set of applications.

This encompasses task synchronization and locking primitives, integrating with multi-core microcontrollers, and managing multiple energy buffers, all within the context of real-time operating systems and batteryless devices.

## REFERENCES

- [1] B. Denby and B. Lucia, "Orbital edge computing: Nanosatellite constellations as a new class of computer system," in *Proceedings of the Twenty-Fifth International Conference on Architectural Support for Programming Languages and Operating Systems*, 2020, pp. 939–954.
- [2] J. Choi, L. Kittinger, Q. Liu, and C. Jung, "Compiler-directed high-performance intermittent computation with power failure immunity," in *2022 IEEE 28th Real-Time and Embedded Technology and Applications Symposium (RTAS)*. IEEE, 2022, pp. 40–54.
- [3] J. Hester and J. Sorber, "The future of sensing is batteryless, intermittent, and awesome," in *Proceedings of the 15th ACM conference on embedded network sensor systems*, 2017, pp. 1–6.
- [4] K. Maeng and B. Lucia, "Adaptive Dynamic Checkpointing for Safe Efficient Intermittent Computing," in *OSDI*, 2018.
- [5] A. Mirhoseini, E. M. Songhori, and F. Koushanfar, "Idetic: A High-level Synthesis Approach for Enabling Long Computations on Transiently-powered ASICs," in *2013 IEEE International Conference on Pervasive Computing and Communications (PerCom)*, 2013, pp. 216–224.
- [6] B. Ransford, J. Sorber, and K. Fu, "Mementos: System Support for Long-running Computation on RFID-scale Devices," in *ASPLOS*, 2011. [Online]. Available: <http://doi.acm.org/10.1145/1950365.1950386>
- [7] J. Hester, K. Storer, and J. Sorber, "Timely Execution on Intermittently Powered Batteryless Sensors," in *SenSys*, 2018.
- [8] H. Jayakumar *et al.*, "QUICKRECALL: A low overhead HW/SW approach for enabling computations across power cycles in transiently powered computers," in *IEEE International Conference on VLSI Design*, 2014.
- [9] K. Maeng and B. Lucia, "Adaptive Low-Overhead Scheduling for Periodic and Reactive Intermittent Execution," in *PLDI*, 2020.
- [10] —, "Supporting Peripherals in Intermittent Systems with Just-in-Time Checkpoints," in *Proceedings of the 40th ACM SIGPLAN Conference on Programming Language Design and Implementation*, ser. PLDI 2019. New York, NY, USA: Association for Computing Machinery, 2019, p. 1101–1116. [Online]. Available: <https://doi.org/10.1145/3314221.3314613>
- [11] FreeRTOS, "FreeRTOS - Market leading RTOS (Real Time Operating System) for embedded systems with Internet of Things extensions." [Online]. Available: <https://freertos.org/>
- [12] "µC/OS RTOS and Stacks." [Online]. Available: <https://weston-embedded.com/micrium/17-micrium/58-micrium-kernels>
- [13] "RTEMS Real Time Operating System (RTOS) — Real-Time and real Free RTOS." [Online]. Available: <https://www.rtems.org/>
- [14] A. Colin and B. Lucia, "Chain: tasks and channels for reliable intermittent programs," in *Proceedings of the 2016 ACM SIGPLAN International Conference on Object-Oriented Programming, Systems, Languages, and Applications*, 2016, pp. 514–530.
- [15] K. Maeng, A. Colin, and B. Lucia, "Alpaca: Intermittent Execution without Checkpoints," *Proc. ACM Program. Lang.*, vol. 1, no. OOPSLA, oct 2017.
- [16] M. Karimi, H. Choi, Y. Wang, Y. Xiang, and H. Kim, "Real-Time Task Scheduling on Intermittently Powered Batteryless Devices," *IEEE Internet of Things Journal*, vol. 8, no. 17, pp. 13 328–13 342, 2021.
- [17] B. Islam and S. Nirjon, "scheduling computational and energy harvesting tasks in deadline-aware intermittent systems," in *IEEE Real-Time and Embedded Technology and Applications Symposium (RTAS)*, 2020.
- [18] —, "Zygarde: Time-Sensitive On-Device Deep Inference and Adaptation on Intermittently-Powered Systems," *Proc. ACM Interact. Mob. Wearable Ubiquitous Technol.*, vol. 4, no. 3, 2020.
- [19] M. Karimi and H. Kim, "Energy Scheduling for Task Execution on Intermittently-Powered Devices," *ACM SIGBED Review*, vol. 17, no. 1, pp. 36–41, 2020.
- [20] V. Kortbeek, K. S. Yildirim, A. Bakar, J. Sorber, J. Hester, and P. Pawelczak, "Time-sensitive intermittent computing meets legacy software," in *Proceedings of the Twenty-Fifth International Conference on Architectural Support for Programming Languages and Operating Systems*, 2020, pp. 85–99.
- [21] N. A. Bhatti and L. Mottola, "harvos: Efficient code instrumentation for transiently-powered embedded sensing," in *Proceedings of the 16th ACM/IEEE International Conference on Information Processing in Sensor Networks*, 2017, pp. 209–219.
- [22] Y. Kim, Y. Lim, and C. Lim, "Liveness-aware checkpointing of arrays for efficient intermittent computing," in *2023 Design, Automation & Test in Europe Conference & Exhibition (DATE)*. IEEE, 2023, pp. 1–6.
- [23] K. S. Yildirim, A. Y. Majid, D. Patoukas, K. Schaper, P. Pawelczak, and J. Hester, "InK: Reactive Kernel for Tiny Batteryless Sensors," in *SenSys*, 2018.
- [24] A. Colin, E. Ruppel, and B. Lucia, "A Reconfigurable Energy Storage Architecture for Energy-harvesting Devices," in *ACM SIGPLAN Notices*, vol. 53, 2018.
- [25] A. Colin and B. Lucia, "Termination Checking and Task Decomposition for Task-Based Intermittent Programs," in *Proceedings of the 27th International Conference on Compiler Construction*, ser. CC 2018. New York, NY, USA: Association for Computing Machinery, 2018, p. 116–127.
- [26] D. Balsamo, A. S. Weddell, G. V. Merrett, B. M. Al-Hashimi, D. Brunelli, and L. Benini, "Hibernus: Sustaining Computation During Intermittent Supply for Energy-Harvesting Systems," *IEEE Embedded Systems Letters*, vol. 7, no. 1, pp. 15–18, 2015.
- [27] M. Karimi, Y. Wang, and H. Kim, "Energy-Adaptive Real-time Sensing for Batteryless Devices," in *2022 IEEE 28th International Conference on Embedded and Real-Time Computing Systems and Applications (RTCSA)*, 2022, pp. 205–211.
- [28] H. R. Mendis, C.-K. Kang, and P.-c. Hsiu, "Intermittent-Aware Neural Architecture Search," *ACM Trans. Embed. Comput. Syst.*, vol. 20, no. 5s, sep 2021. [Online]. Available: <https://doi.org/10.1145/3476995>
- [29] J. Hester, L. Sitanayah, and J. Sorber, "Tragedy of the Coulombs: Federating Energy Storage for Tiny, Intermittently-Powered Sensors," in *Proceedings of the 13th ACM Conference on Embedded Networked Sensor Systems*, ser. SenSys '15. New York, NY, USA: Association for Computing Machinery, 2015, p. 5–16. [Online]. Available: <https://doi.org/10.1145/2809695.2809707>
- [30] H. Jayakumar, A. Raha, J. R. Stevens, and V. Raghunathan, "Energy-Aware Memory Mapping for Hybrid FRAM-SRAM MCUs in Intermittently-Powered IoT Devices," *ACM Trans. Embed. Comput. Syst.*, vol. 16, no. 3, apr 2017. [Online]. Available: <https://doi.org/10.1145/2983628>
- [31] K. Wardega, W. Li, H. Kim, Y. Wu, Z. Jia, and J. Hu, "Opportunistic communication with latency guarantees for intermittently-powered devices," in *2022 Design, Automation & Test in Europe Conference & Exhibition (DATE)*. IEEE, 2022, pp. 1093–1098.
- [32] J. Hester, N. Tobias, A. Rahmati, L. Sitanayah, D. Holcomb, K. Fu, W. P. Burleson, and J. Sorber, "Persistent Clocks for Batteryless Sensing Devices," *ACM Trans. Embed. Comput. Syst.*, vol. 15, no. 4, aug 2016. [Online]. Available: <https://doi.org/10.1145/2903140>
- [33] H. Choi, M. Karimi, and H. Kim, "Chain-Based Fixed-Priority Scheduling of Loosely-Dependent Tasks," in *2020 IEEE 38th International Conference on Computer Design (ICCD)*, 2020, pp. 631–639.
- [34] H. Sobhani, H. Choi, and H. Kim, "Timing Analysis and Priority-driven Enhancements of ROS 2 Multi-threaded Executors," in *2023 IEEE 29th Real-Time and Embedded Technology and Applications Symposium (RTAS)*. IEEE, 2023, pp. 106–118.
- [35] H. Kim, S. Yi, W. Jung, and H. Cha, "A decentralized approach for monitoring timing constraints of event flows," in *2010 31st IEEE Real-Time Systems Symposium*. IEEE, 2010, pp. 327–336.
- [36] C. Delgado and J. Famaey, "Optimal energy-aware task scheduling for batteryless iot devices," *IEEE Transactions on Emerging Topics in Computing*, vol. 10, no. 3, pp. 1374–1387, 2021.
- [37] J. Regehr, "Scheduling tasks with mixed preemption relations for robustness to timing faults," in *23rd IEEE Real-Time Systems Symposium, 2002. RTSS 2002*. IEEE, 2002, pp. 315–326.
- [38] E. Bini and G. C. Buttazzo, "Measuring the performance of schedulability tests," *Real-Time Systems*, vol. 30, no. 1-2, pp. 129–154, 2005.